Supplementary Information

Title:

Millimetre Wave with Rotational Orbital Angular Momentum

Chao Zhang* Lu Ma

Labs of Avionics, School of Aerospace Engineering,

Tsinghua University, Beijing, 100084, P. R. China

*To whom correspondence should be addressed; E-mail: zhangchao@tsinghua.edu.cn.

Supplementary Notes

Supplementary Notes 1: Descriptions of the experiments and the methods

In the simulations, we find that the vortex of the radio wave is equivalent by field superposition. The radiation field rotates only during propagation, and it does not rotate at a specific point in a fixed distance. We name this type of OAM radio wave as the stationary OAM field. In this case, the entire energy ring vertical to the radiation axis should be received via a ring-shaped antenna (or antenna array) in the space domain to distinguish radio waves of different OAM modes. With the distance increasing, such a ring-shaped antenna becomes impossibly large due to the diverging beam angle. However, if the OAM wave can rotate at the transmitter, then its reception with a single antenna at a fixed point is possible. The entire energy ring can be received sequentially in the time domain. The frequency shift occurs proportionally to the rotational speed. To ensure that the polarization remains unchanged in the rotational OAM wave, only the SPP is rotated with the electrical machine, rather than the transmitting antenna. The rotational OAM wave can be considered a dynamic OAM field and can produce different frequency shifts for different OAM modes. Moreover, the signals with different frequency shifts are found to be in the form of Orthogonal Frequency Division Multiplex (OFDM).

Supplementary Figures

Supplementary Figure 1

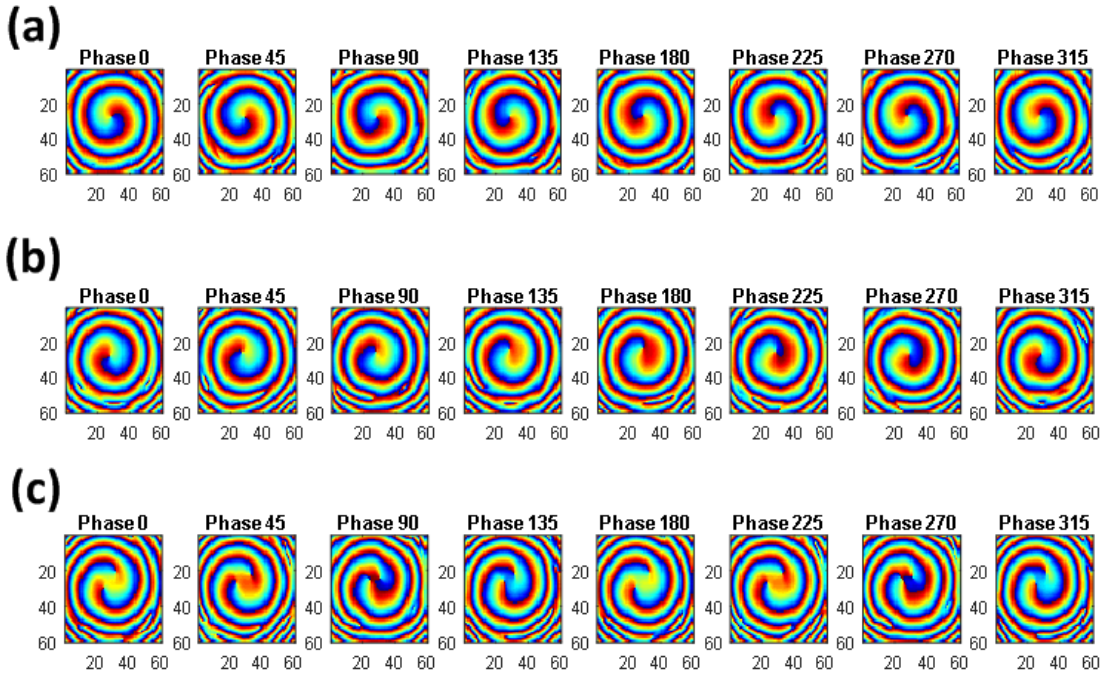

Supplementary Figure 1 Phase measurements of the OAM waves with different SPPs at 8 different azimuth angles, i.e., 0^{o}, 45^{o}, 90^{o}, 135^{o}, 180^{o}, 225^{o}, 270^{o}, and 315^{o}. **(a)** SPP with the OAM mode of -1. **(b)** SPP with the OAM mode of +1. **(c)** SPP with the OAM mode of +2.

Supplementary Figure 2

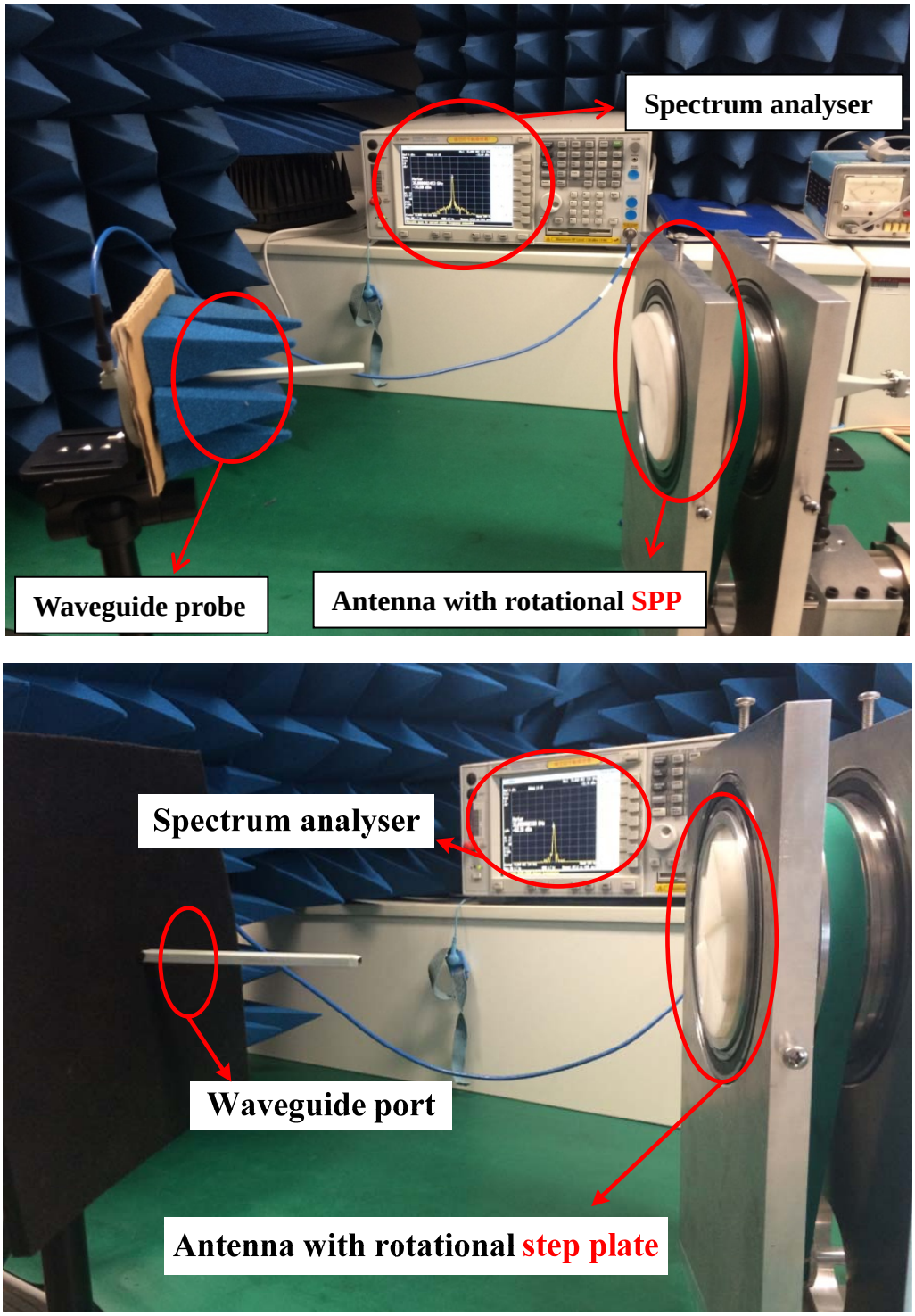

Supplementary Figure 2 Experimental apparatus of the frequency shift measurements with two types of phase plates, i.e., the SPP and step plate, corresponding to Fig. 3a.

Supplementary Figure 3

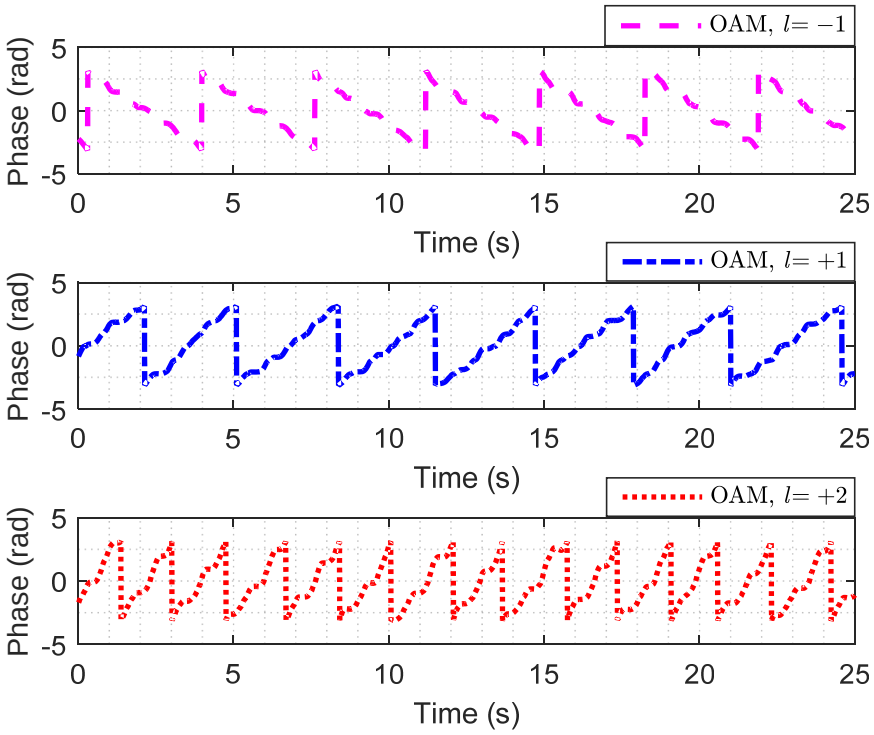

Supplementary Figure 3 The measured phase variation curves corresponding to Fig. 2c.

Supplementary Figure 4

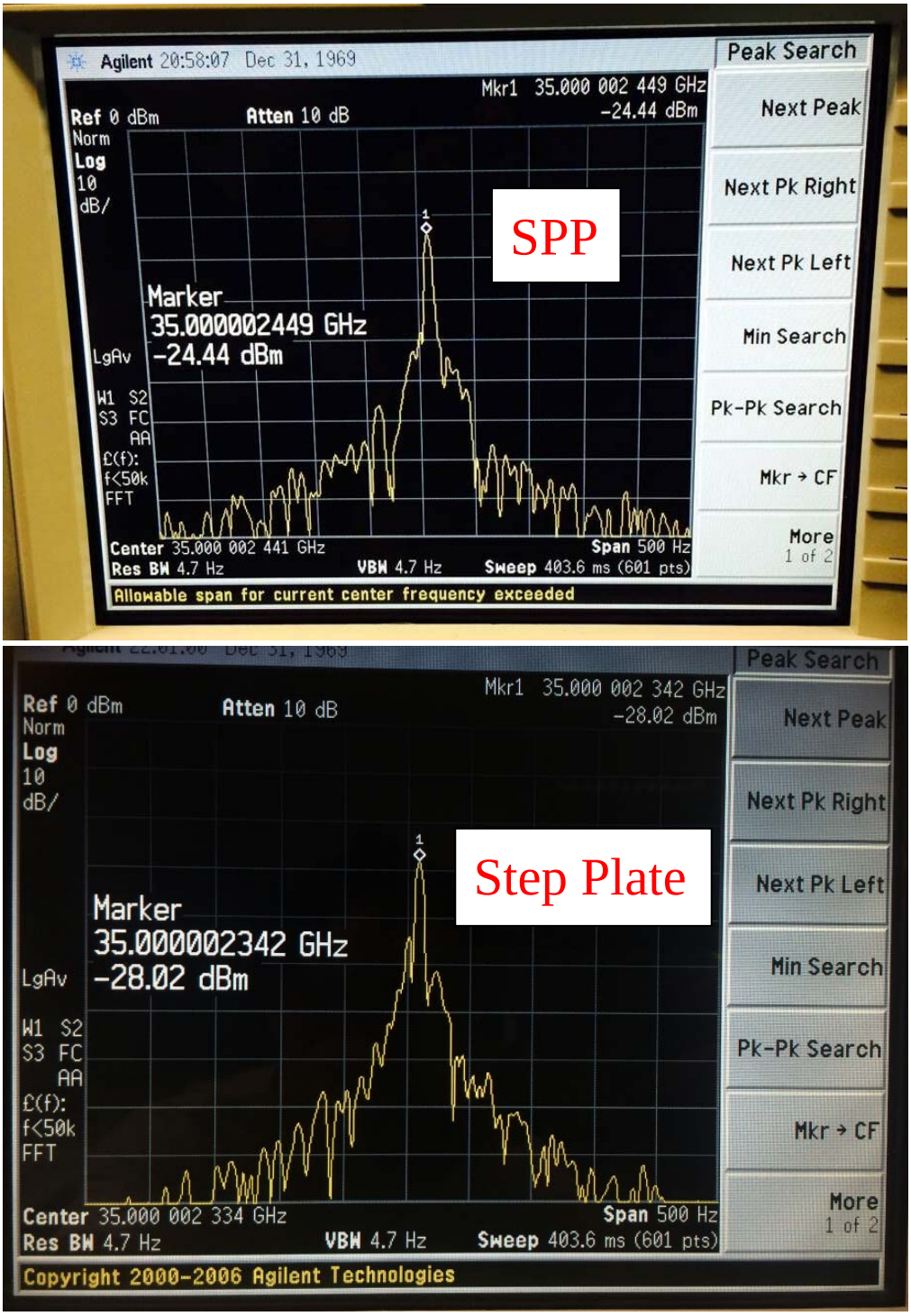

Supplementary Figure 4 Data acquisition using the spectrum analyser for the OAM mode of +1 at the rotation speed of 7.2 (r/s).

Supplementary Figure 5

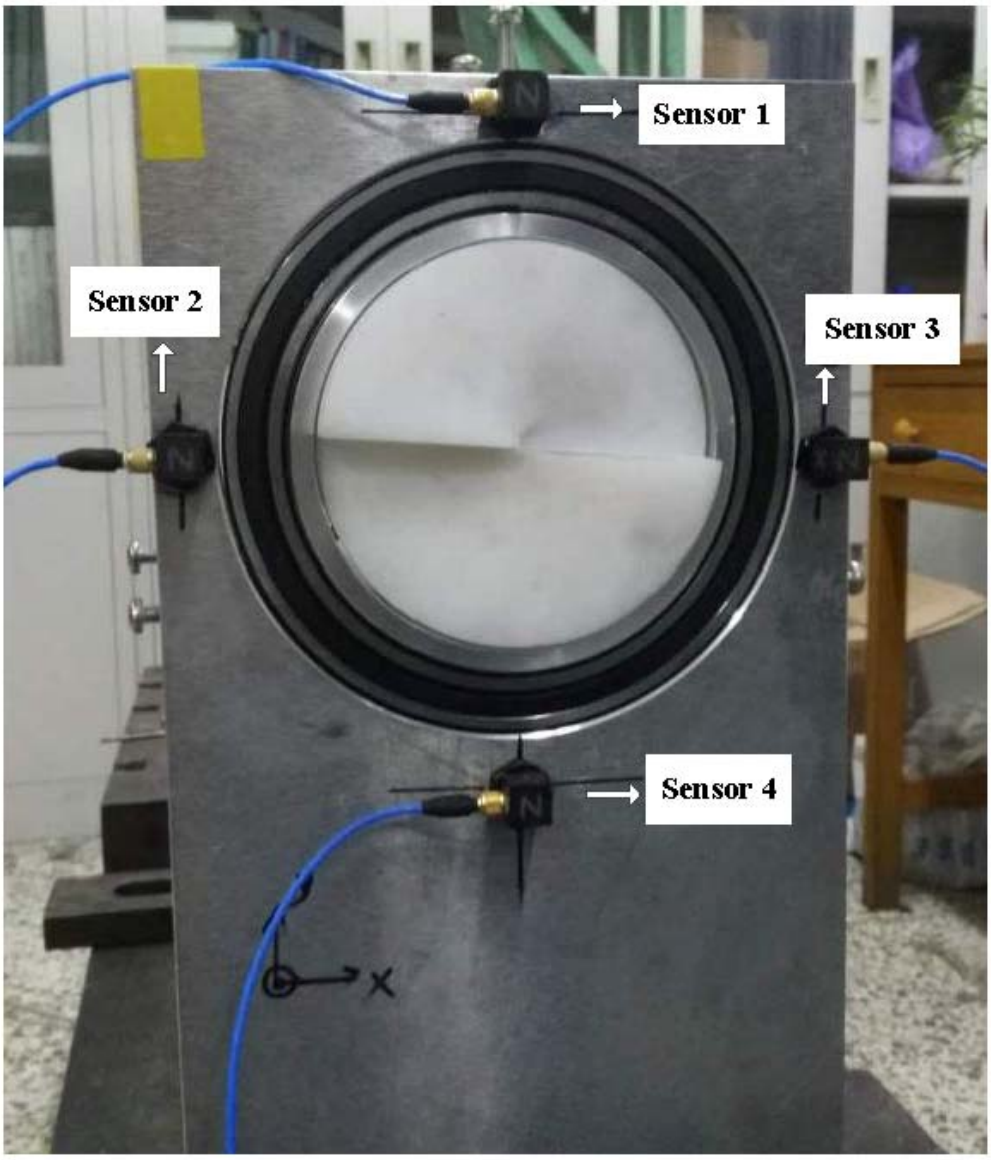

Supplementary Figure 5 Vibration measurements using tri-axis accelerometers of model 356A16 manufactured by PCB Piezotronics Inc.

Supplementary Table

Supplementary Table 1 The frequency detected for the rotational SPP shown in Fig. 3d. Note that at the low mechanical rotating speed in the experiment, the generated frequency shift is small and that only the last two digits vary.

	Rotation speed (r/s)			
	0	2.4	4.8	7.2
OAM mode	Frequency with associated error detected by spectrum analyser (Hz)			
l = 0	35000 002 441 ± 0.9	35000 002 441 ± 0.8	35000 002 441 ± 0.9	35000 002 441 ± 1.3
l = -1	35000 002 441 ± 1	35000 002 438 ± 1	35000 002 435 ± 1.1	35000 002 433 ± 1.1
l = +1	35000 002 441 ± 1.1	35000 002 444 ± 0.9	35000 002 447 ± 1.3	35000 002 449 ± 1.2
l = +2	35000 002 441 ± 0.9	35000 002 446 ± 0.7	35000 002 451 ± 0.5	35000 002 456 ± 1.4

Supplementary Table 2 The frequency detected for the rotational step plate shown in Fig. 3d. Note that, these data were not acquired on the same day as those given in supplementary table 1. As a result, the static frequency is different from that of Supplementary Table 1 due to many factors, e.g. the environment temperature, etc.

	Rotation speed (r/s)			
	0	2.4	4.8	7.2
OAM mode	Frequency with associated error detected by spectrum analyser (Hz)			
l = 0	35000 002 334 ± 1	35000 002 334 ± 1.5	35000 002 334 ± 0.9	35000 002 334 ± 1.1
l = -1	35000 002 334 ± 1	35000 002 331 ± 1.3	35000 002 329 ± 1.8	35000 002 327 ± 2.1
l = +1	35000 002 334 ± 1.5	35000 002 337 ± 1.5	35000 002 339 ± 2	35000 002 342 ± 1.5
l = +2	35000 002 334 ± 1.2	35000 002 339 ± 1.9	35000 002 344 ± 1.3	35000 002 349 ± 1.3

Supplementary Table 3 The polarization detected for the rotational step plate shown in Fig. 4b. At each polarization direction, 5000 points are measured and averaged. The rotation speed is 2.4 (r/s).

	Direction of polarization (degree)		
	0	45	90
OAM mode	Amplitude with associated error detected by spectrum analyser (dB)		
l = -1	-43.0256 ± 1.9777	-46.2694 ± 1.7825	-63.6465 ± 5.3014
l = +1	-42.7332 ± 1.8842	-45.3967 ± 2.2149	-61.8319 ± 4.9192
l = +2	-50.9554 ± 5.1140	-53.7091 ± 4.5899	-65.0531 ± 6.3888

Supplementary Table 4 The effective values of displacements measured with tri-axis accelerometers of model 356A16 manufactured by PCB Piezotronics Inc.

	The effective values of displacements (mm)			
	Sensor 1	Sensor 2	Sensor 3	Sensor 4
X-axis	0.08477566939799	0.06390757635507	0.07007711433296	0.03812078989415
Y-axis	0.05708462370474	0.02853160809574	0.05173361542962	0.04910758087534
Z-axis	0.05015614491186	0.03180416516017	0.0333528949554	0.02441965928097